Journal of Chromatography A, 1217 (2010) 7573–7578

Contents lists available at ScienceDirect

Journal of Chromatography A

journal homepage: www.elsevier.com/locate/chroma

pH transients in hydroxyapatite chromatography columns—Effects of operating conditions and media properties

Laura Dattolo, Emily L. Keller, Giorgio Carta*

Department of Chemical Engineering, University of Virginia, 102 Engineers' Way, Charlottesville, VA 22904-4741, USA

ARTICLE INFO

Article history:
Received 4 August 2010
Received in revised form
29 September 2010
Accepted 4 October 2010
Available online 11 October 2010

Keywords:
Hydroxyapatite
pH transitions
Modeling
Managing

ABSTRACT

pH transitions occur in hydroxyapatite (HAP) columns that are subject to step changes in salt concentration, which have been shown to be controlled by proton exchange on the HAP surface. The pH temporarily decreases before gradually returning to the feed value when the salt concentration increases, potentially compromising the stability of the HAP when either the magnitude or duration of the pH drop is excessive. The opposite happens when the salt concentration decreases. In this work we address the effects of several key variables: the flow rate, the particle size, the use of salt gradients instead of steps, the use of different co-buffers, the surface area of the HAP, and the use of a slightly alkaline wash prior to increasing the salt concentration. Flow rate and particle size were found to have virtually no effect, demonstrating that the pH transitions are equilibrium rather than kinetically driven. Salt gradients resulted in smaller pH drops compared to steps since the exchanged protons are diluted over the gradient volume. MES and histidine used as co-buffers were effective at reducing the duration of the pH transitions but did not affect their magnitude. The same result was found when comparing HAP samples with different surface areas, with the lower surface area HAP yielding much shorter duration but similar pH drops and rises. Finally, washing the HAP column with a pH 7.5 buffer prior to the salt step was found to dramatically reduce the subsequent pH drop. In general, there was good agreement between these results and predictions based on our previously developed model.

1. Introduction

Hydroxyapatite (HAP) is used extensively in process scale chromatography separations of proteins and other biomolecules (e.g. see ref. [1–8]). In this role, HAP is thought to function through the combined effects of calcium and phosphate groups present on exposed HAP crystal surfaces, which provide unique selectivity and afford the ability to separate complex mixtures [9–13]. Although these groups do not define discrete surface elements, they are sometimes referred to as C-sites and P-sites, respectively. In general, cationic proteins are adsorbed mainly through interactions with phosphate groups primarily as a result of electrostatic interactions. Anionic proteins, on the other hand, are adsorbed mainly through interactions with surface calcium primarily through the formation of coordination complexes between carboxyl and phosphate groups on the protein surface and exposed calcium on the surface of the HAP crystals [14,15].

Despite the effectiveness of HAP as a stationary phase, an operational concern is the solubility of HAP at pH values below 6.5 [16–18], which requires careful pH control in order to avoid loss of column stability [19]. Unfortunately, this is not always easy to achieve for two main reasons. Firstly, the mobile phases that are desirable for separation frequently have relatively low buffering capacity. Secondly, as noted by Cummings [20], even though the mobile phase is buffered, substantial pH excursions can occur in HAP columns in response to step changes in salt concentration. As shown by Cummings [20] and in our prior work [21], the pH temporarily decreases below the feed value when the salt concentration increases and increases above the feed value when the salt concentration is decreased. The intensity and duration of these transients varies with buffer type and with the magnitude of the salt concentration step, but in extreme cases the pH can drop substantially creating conditions where the HAP stability is potentially compromised. Phosphate adsorption and release from the HAP surface were also found to occur and the interplay of these two adsorption phenomena was found to be responsible for the complex patterns of pH observed experimentally [21]. A phenomenological model taking into account the reversible uptake of sodium ions by the P-sites and binding of phosphate ions by the C-sites was found to be in agreement with the experiments.

The objective of the present work is to assess quantitatively the effects of various operating conditions on the pH transients of

* Corresponding author at: Department of Chemical Engineering, University of Virginia, School of Engineering and Appl. Science, 102 Engineers' Way, P.O. Box 400741, Charlottesville, VA 22904-4741, USA. Tel.: +1 434 924 6281; fax: +1 434 982 2658.
E-mail address: gc@virginia.edu (G. Carta).

0021-9673/$ – see front matter © 2010 Elsevier B.V. All rights reserved.
doi:10.1016/j.chroma.2010.10.026

HAP columns with an emphasis on determining approaches that can minimize acidic conditions and thus extend column lifetime. Various potential approaches are explored experimentally and are analyzed through our previously developed model. For simplicity, our work is done without any applied protein sample, since, in practice, we expect that the general features would be the same except for extremely concentrated protein solutions.

2. Experimental

CHT® Ceramic Hydroxyapatite Type I and Type II were obtained from Bio-Rad Laboratories (Hercules, CA, USA). According to the manufacturer, both types have a bulk density of 0.63 g/ml [19]. The principal difference is thus pore size, which is reported as 60–80 nm for Type I and 80–100 nm for Type II. Correspondingly, Type I has a larger surface area and generally a larger protein binding capacity compared to that of Type II [22]. Two different samples with different particle size, 40 ± 4 and 80 ± 4 μm, were obtained. Samples of each material were packed in 10 mm × 100 mm Tricorn glass chromatography columns from GE Healthcare (Piscataway, NJ, USA) to a packed bed height of 9–11 cm using the procedure recommended by Bio-Rad. This procedure gave reproducible packing with reduced HETP values (h = HETP/d_p where d_p is the particle diameter) between 4 and 12 based on the conductivity response to a small pulse of NaCl in the phosphate running buffer at 4 ml/min. The column void volume was determined from the chromatographic retention of glucose, which gave a total column porosity $\varepsilon = 0.8$. The experiments were conducted with an AKTA Explorer 10 chromatographic workstation from GE Healthcare.

The buffer solutions used in this work were prepared as follows. Phosphate buffers were prepared by dissolving preset amounts of 5 mM Na_2HPO_4 and NaCl in water and then adjusting the pH to 6.5 with the addition of concentrated phosphoric acid. MES/phosphate and histidine/phosphate buffers were prepared by adding MES acid and histidine base, respectively, to solutions containing 5 mM Na_2HPO_4 and NaCl and adding concentrated phosphoric acid to attain a pH of 6.5. MES solutions for the surface neutralization step were prepared by adding 10 mM MES to 5 mM Na_2HPO_4 and titrating the solution to pH 7.5 with 1 M NaOH. For each experiment, the column was first equilibrated with approximately 20 column volumes of the initial buffer and then subjected to step or linear gradient changes from low to high salt and vice versa. The effluent conductivity was determined on line using the AKTA system monitor while the pH was determined by collecting 4 ml fractions (~0.5 column volumes) and measuring with a pH meter using a calibrated combination probe.

3. Experimental results

Fig. 1 shows the pH transitions observed at different flow rates for 500 mM positive and negative NaCl steps with 5 mM Na_2HPO_4 buffers at pH 6.5 with the Type I media. The conductivity traces are practically indistinguishable. In all three cases, the pH temporarily decreases during the positive salt step and temporarily increases during the negative salt step. As discussed in our previous paper [21], the pH drop occurs as a result of the exchange of Na^+ ions for surface bound protons coupled with the simultaneous adsorption of free phosphate ions on the HAP surface. The opposite happens during the negative salt step. In this case Na^+ bound to surface phosphate groups is exchanged back for protons from the mobile phase while free phosphate is released from the surface. The flow rate independence indicates that the pH transitions are driven by equilibrium rather than by kinetic factors even though the residence time is as low as 60 s. The result suggests that operating at high flow rates is beneficial since, although the pH transitions are the same when plotted versus the number of column volumes passed through, CV, the time of exposure of the HAP to the potentially damaging low pH conditions is reduced in inverse proportion to the flow rate.

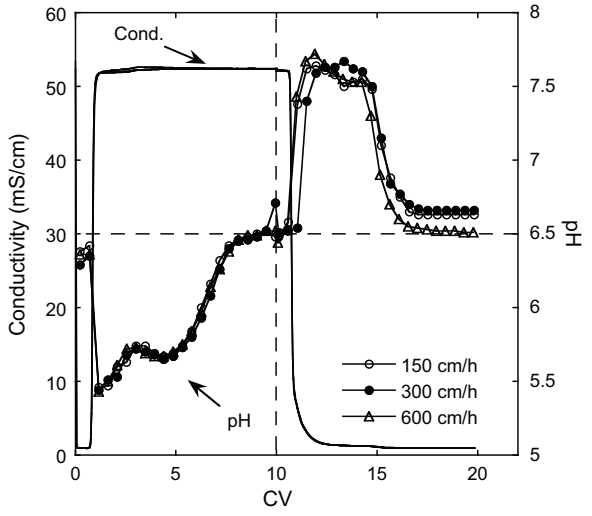

Fig. 1. Effect of mobile phase velocity on pH transients in Type I CHT column (40 μm) for positive and negative 0–500 mM NaCl steps in 5 mM Na_2HPO_4 at pH 6.5.

Fig. 2 compares the results obtained at 300 cm/h with 40 and 80 μm particles for otherwise identical conditions. The conductivity traces are again nearly coincident. The pH profiles are also virtually the same suggesting that the surface phenomena responsible for the generation of the pH transients are independent of particle size and that diffusion of the buffer species in the particles is sufficiently fast to maintain near local equilibrium conditions. Cummings and Snyder [23] have reported that CHT columns disrupted by exposure to low pH show evidence that fines are formed. It can be assumed that these fines can plug the interparticle space and, thus, cause the increased pressure observed experimentally for degraded CHT columns [22]. Since columns packed with larger diameter particles are likely to be less prone to plugging, for the same pH transitions and damage caused by the low pH conditions, they can be expected to have a somewhat longer lifetime.

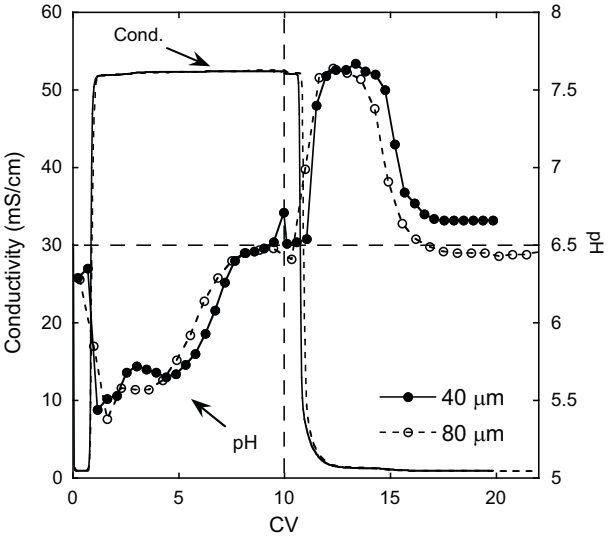

Fig. 2. Effect of particle size on pH transients in Type I CHT column for positive and negative 0–500 mM NaCl steps in 5 mM Na_2HPO_4 at pH 6.5 at 300 cm/h.

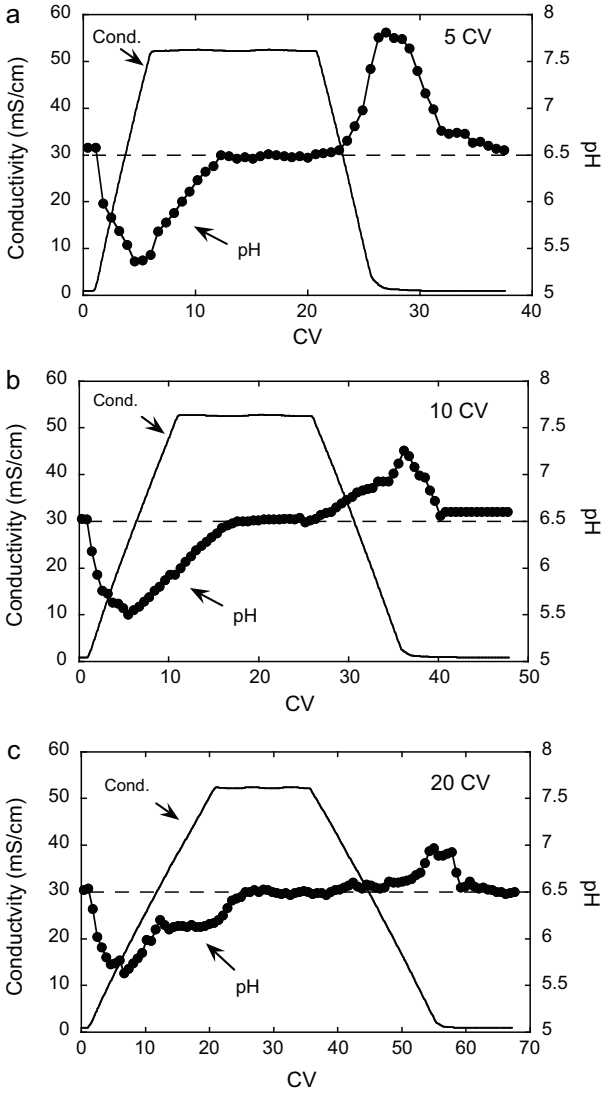

Fig. 3. pH transients in Type I CHT column (40 μm) for positive and negative 0–500 mM NaCl gradients in 5 mM Na_2HPO_4 at pH 6.5 and 300 cm/h. The gradient durations are 5, 10, and 20 CV for a, b, and c, respectively.

Fig. 3 shows the Type I CHT response to positive and negative 500 mM NaCl gradients of different durations using 5 mM Na_2HPO_4 buffers at pH 6.5. The gradient durations are expressed in terms of the number of column volumes, CV. An intermediate high-salt hold was used between the gradients. As seen in Fig. 3, the five CV gradients give pH transients very similar to those obtained with the corresponding steps. However, increasing the gradient duration to 10 or 20 CV substantially dampens the pH drop during the positive gradient and almost completely eliminates the pH rise during the negative gradient. Since the HAP solubility is a highly non-linear function of pH (e.g. see Fig. 1 in ref. [21]), even a relatively small reduction in the pH minimum is expected to provide substantial benefits. The underlying reasons for the pH drop are the same as those responsible for that obtained with the steps. However, with the gradient, the Na^+-H^+ exchange on the HAP surface occurs gradually so that a less severe instantaneous depletion of Na^+ from the running buffer occurs. In turn, the smaller pH drop can be expected to result in less disruption of the CHT.

Fig. 4 illustrates the effect of co-buffers added to 5 mM Na_2HPO_4 buffers at pH 6.5 with 500 mM NaCl steps for a Type I column. In our previous work [21] we showed that 20 mM MES can be used to reduce the duration of the pH drop during the positive salt step.

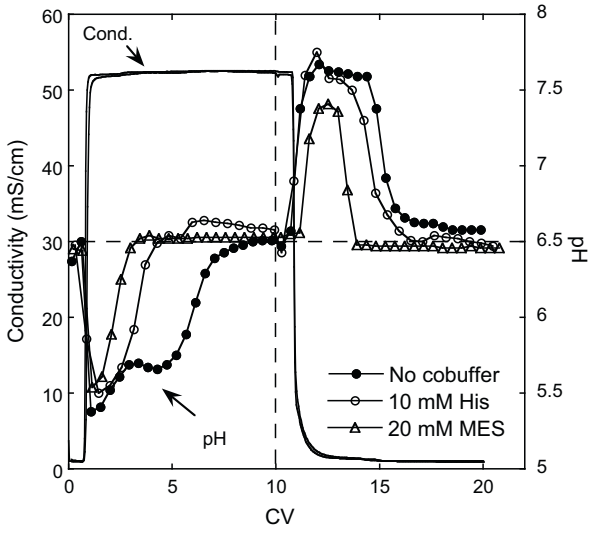

Fig. 4. Effect of co-buffers on pH transients in Type I CHT column (40 μm) for positive and negative 0–500 mM NaCl steps in 5 mM Na_2HPO_4 at pH 6.5 at 300 cm/h. The MES data are from ref. [21].

Although MES is effective, as seen in Fig. 4 as little as 10 mM histidine also accomplishes a substantial reduction. In all three cases (without co-buffer, with 10 mM His, and with 20 mM MES), the pH reaches a minimum around 5.4. However, the duration of the pH drop is profoundly different, decreasing from about 10 CV without co-buffer to about 4 CV with 10 mM His to about 3 CV with 20 mM MES. The mechanism by which these co-buffers function is similar. Both have pK_a's around 6. Thus, they can accept a substantial fraction of the protons released from the HAP surface when the NaCl concentration is increased. Of course, His could be expected to bind to the phosphate groups on the HAP surface in competition with Na^+. However, this phenomenon seems not to have adverse effects on the pH transitions, likely because Na^+ is in excess in the high salt buffer and little His binding occurs.

Fig. 5 shows the pH transitions obtained with Type I CHT when the column is temporarily exposed to a pH 7.5 MES/phosphate buffer prior to a step to 5 mM Na_2HPO_4 with 500 mM NaCl at pH 6.5. As seen in this figure, increasing the duration of the pH 7.5 step dramatically reduces the pH drop during the subsequent NaCl step. As discussed in our prior work [21], the HAP is acidic because of surface-exposed phosphate groups. Since the pK_a of these groups is around 7.2, similar to the pK_a of free phosphate, protons are released when the HAP is exposed to high salt solutions at pH 6.5 causing the pH to drop. On the other hand, as seen in Fig. 5, exposing the HAP to a pH 7.5 buffer removes most of these protons and replaces them with Na^+. As a result, when NaCl is added in the subsequent step, little additional H^+ is released so that only a small drop in pH is observed. Such an approach has been described recently by Cummings and Snyder [24] as a way to improve column lifetime and termed "surface neutralization step", or SNS (patent pending, Bio-Rad Laboratories). As seen in Fig. 5, it is obvious that to be effective, a sufficient amount of pH 7.5 buffer is needed to dampen the pH drop. For these conditions, 2 CV's of pH 7.5 buffer still give a minimum pH of about 5.7. However, the pH drops to only about 6.1 with 5 CV's and to only about 6.2 with 10 CV's. Note that with 10 CV's the column is nearly completely equilibrated with the pH 7.5 buffer indicating that the maximum neutralization of the surface protons possible with this buffer has been achieved.

Figs. 6 and 7 compare the results obtained with Type II CHT with 500 mM NaCl steps and gradients, respectively, using 5 mM Na_2HPO_4 buffers at pH 6.5 with those obtained with Type I CHT for otherwise identical conditions. As seen in Fig. 6 for step changes, the

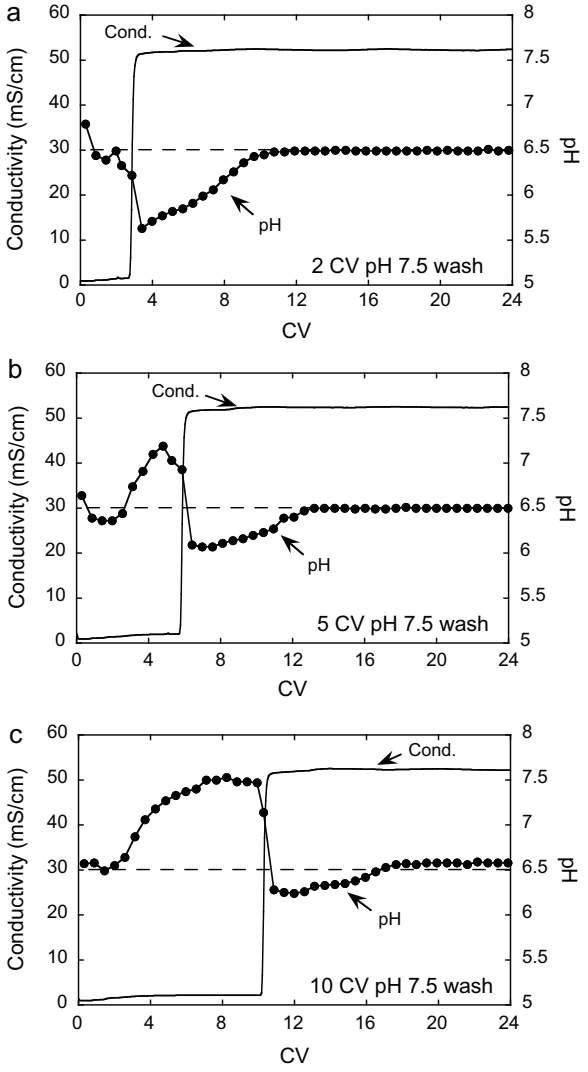

Fig. 5. pH transients in Type I CHT column (40 μm) for positive 0–500 mM NaCl steps in 5 mM Na_2HPO_4 at pH 6.5 and 300 cm/h following a column wash with 10 mM MES and 5 mM Na_2HPO_4 at pH 7.5 for (a) 2 CV, (b) 5 CV, and (c) 10 CV.

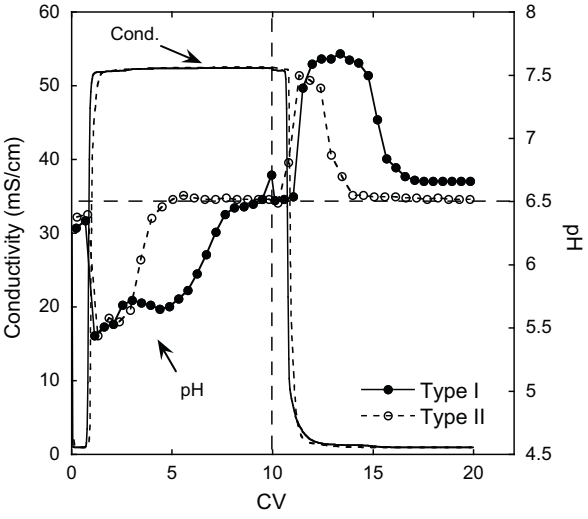

Fig. 6. Comparison of pH transients in Type I and Type II CHT columns (40 μm) for positive and negative 0–500 mM NaCl steps in 5 mM Na_2HPO_4 at pH 6.5 and 300 cm/h.

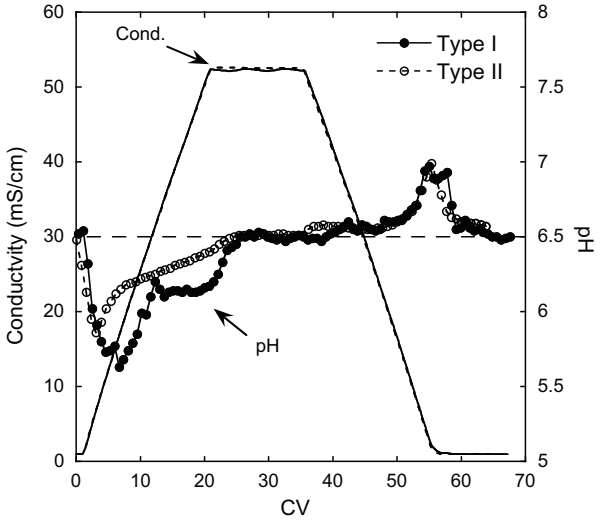

Fig. 7. Comparison of pH transients in Type I and Type II CHT columns (40 μm) for 20 CV positive and negative 0–500 mM NaCl gradients in 5 mM Na_2HPO_4 at pH 6.5 and 300 cm/h.

magnitude of the pH transitions is nearly the same for both types and in both directions. However, the duration of both pH transitions is much shorter for Type II and, in fact, nearly exactly equal to one-half of the duration of the Type I transitions. Since, based on the protein binding capacity, the Type II surface area is about one-half of that of Type I, this result suggest that the pH transitions are directly related to the HAP surface area. The salt gradient behavior shows a similar duration but a reduced pH drop for Type II compared to Type I. This behavior also suggests a direct dependence on the surface area. In this case, however, a different minimum pH is reached with Type II since a smaller amount of protons is released during the positive NaCl gradient (approximately equal to one-half of that released by Type I) and this smaller amount is distributed over the same gradient volume.

4. Model predictions

A simple phenomenological model was developed to describe the HAP pH transients in our previous work [21]. The model assumes that Na^+ ions are exchanged for protons on exposed phosphate groups, while free phosphate is reversibly adsorbed on exposed surface-bound calcium ions by a site sharing mechanism. Accordingly, phosphate is adsorbed when the pH drops and divalent phosphate is converted to monovalent phosphate and is released when the pH rises and phosphate become divalent. Other negatively charged species are assumed to be indifferent to HAP. Finally, the model assumes local equilibrium between the mobile phase and the HAP surface and mimics band broadening due to axial dispersion using a finite difference numerical algorithm. Model parameters were determined in our prior work by data fitting.

In general, a numerical solution was found necessary. However, certain important features, such as the minimum pH attained during a positive salt step, can be predicted analytically. Neglecting axial dispersion, the solution in this case comprises an initial wave corresponding to the propagation of unretained species that moves through the column at the mobile phase velocity. As shown in [21], across this wave front the Na^+ and H^+ concentrations satisfy the equality:

$$\frac{C^{I}_{Na^+}}{C^{I}_{H^+}} = \frac{C^{II}_{Na^+}}{C^{II}_{H^+}} \quad (1)$$

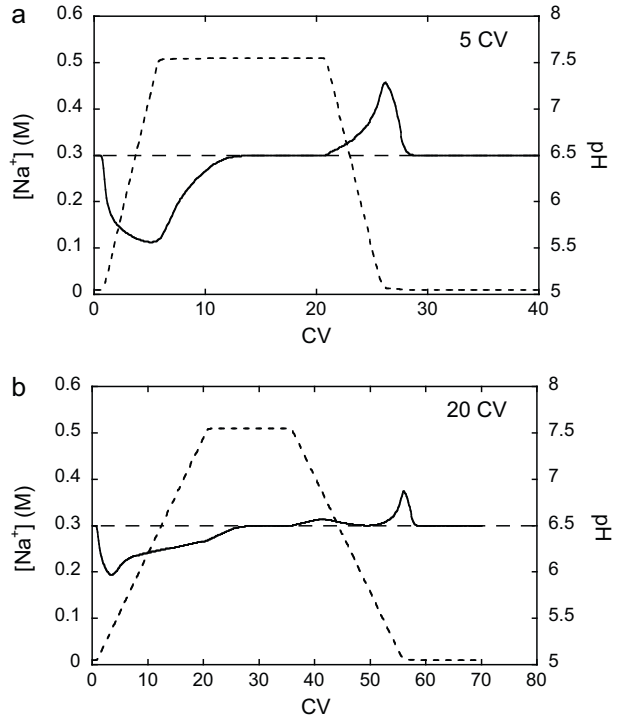

Fig. 8. Predicted pH transients in Type I CHT column (40 μm) for positive and negative 0–500 mM NaCl gradients in 5 mM Na_2HPO_4 at pH 6.5 and 300 cm/h for (a) 5 CV gradient and (b) 20 CV gradient based on the model in ref. [21]. Conditions simulated correspond to those of Fig. 3a and c.

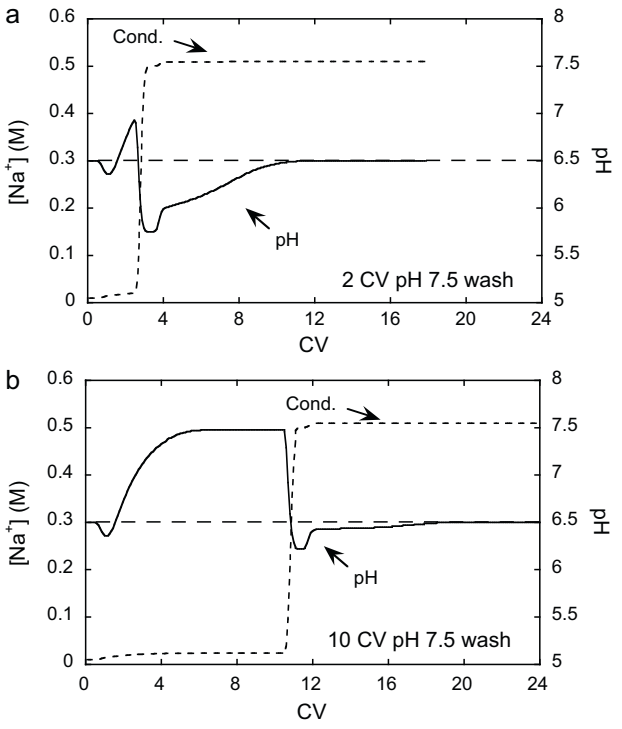

Fig. 9. Predicted pH transients in Type I CHT column (40 μm) for positive 0–500 mM NaCl steps in 5 mM Na_2HPO_4 at pH 6.5 and 300 cm/h following a column wash with 10 mM MES and 5 mM Na_2HPO_4 at pH 7.5 for (a) 2 CV and (b) 10 CV based on the model in ref. [21]. Conditions simulated correspond to those of Fig. 5a and c.

where C_i is the molar concentration of ion i and I and II indicate values immediately downstream and immediately upstream of the front, respectively. For the NaCl steps in Figs. 1, 2, 4, and 6, $C^{I}_{Na^+} = 0.02$ M and $C^{I}_{H^+} \sim 10^{-6.5}$ M. Because of electroneutrality, we have:

$$C^{II}_{Na^+} = (C^{II}_{Cl^-} + C^{II}_{OH^-} + C^{II}_{H_2PO_4^-} + 2C^{II}_{HPO_4^{2-}}) - C^{II}_{H^+} \quad (2)$$

Since Cl^- is in large excess, we have $C^{II}_{Na^+} \sim C^{II}_{Cl^-}$. Thus,

$$C^{II}_{H^+} \sim \frac{C^{I}_{H^+}}{C^{I}_{Na^+}} C^{II}_{Cl^-} = \frac{10^{-6.5}}{0.02} \times 0.5 = 10^{-5.1} \text{ M} \quad (3)$$

or pH ∼ 5.1. Consistent with the experimental observations, this result is independent of flow rate, particle size, co-buffer, and HAP type. A different result is predicted, however, if the NaCl step follows a dilute pH 7.5 buffer. In this case, when the HAP column is completely saturated with the pH 7.5 buffer, as in Fig. 5c, we have $C^{I}_{Na^+} = 0.0238$ M and $C^{I}_{H^+} \sim 10^{-7.5}$ M. Thus, $C^{II}_{H^+} \sim C^{I}_{H^+} C^{II}_{Cl^-} / C^{I}_{Na^+} = 10^{-7.5} \times 0.5/0.0238 = 10^{-6.2}$ M, or pH = 6.2 in good agreement with the results in Fig. 5c. The effect of surface area on the duration of the pH transitions is also predictable with simple calculations. While the minimum pH is independent, the duration is predicted to be proportional to the amount of exchangeable protons, which, in turn, varies with surface area. For Type I, as seen in Fig. 6, the front bringing the pH back to 6.5 following the salt step emerges at an average of about 6.6 CV. Theoretically, as shown in out prior work, this front emerges from the column when:

$$CV = \varepsilon + (1 - \varepsilon)\frac{\Delta q_{Na^+}}{\Delta C_{Na^+}} \quad (4)$$

where q_i is the adsorbed concentration of ion i and △ indicates the difference between values upstream and downstream of this front. Thus, for Type I we have $\Delta q_{Na^+}/\Delta C_{Na^+} = (6.6 - 0.8)/(1 - 0.8) = 29$. Accordingly, since ε and ΔC_{Na^+} are the same for Type I and Type II and the surface area of Type II is about one half that of Type I, the Type II pH front should emerge in CV ∼ 0.8 + (1 − 0.2) × 29/2 = 3.7, which is in good agreement with the experimental result for Type II.

Other features of the pH transitions, including the effects of co-buffers and of non-uniform initial conditions, can be predicted through numerical calculations as shown in our prior work [21]. For the sake of brevity, only two examples are shown here. The first, given in Fig. 8 shows the numerically predicted profiles for 5 and 20 CV gradients. The second, neglecting activity coefficient corrections, given in Fig. 9 shows the predicted profiles for the case where a pH 7.5 dilute buffer step precedes the 500 mM NaCl pH 6.5 step. In both cases, the numerically predicted results are in good agreement with the experimental ones (cf. Fig 3a and b and Fig. 5a and c, respectively) confirming the ability to use the model to select *a priori* conditions where pH transients can be minimized. The predictions for step changes can be found in ref. [21].

5. Conclusions

The pH transitions that occur in hydroxyapatite chromatography columns subject to salt steps are driven largely by the equilibrium between the mobile phase components and the HAP surface. Accordingly, the pH transitions are independent of flow rate (150–600 cm/h) and particle size (40 and 80 μm). The critical parameter determining the magnitude of the pH transitions is the value of ratio C_{Na^+}/C_{H^+} that exists before and after the salt step. This parameter determines the extent of proton release from the HAP surface and the minimum and maximum pH values attained during positive and negative salt steps, respectively. Comparing CHT Type I and II confirms this conclusion. For the same C_{Na^+}/C_{H^+}, the intensity of the pH transitions is the same but their duration is much shorter for Type II since the latter has a much smaller surface area and hence a smaller amount of exchangeable surface protons. Several possibilities are suggested to reduce the duration

and intensity of the pH transitions. The duration can be reduced substantially using co-buffers such as MES or histidine that provide effective buffering. The intensity can be reduced applying salt gradients instead of salt steps or by neutralizing the HAP surface with a very slightly alkaline buffer (e.g. pH 7.5) prior to the salt step. The effectiveness of these approaches at reducing the magnitude and duration of the pH transitions can be predicted by the model presented in ref. [21], which also takes into account the reversible adsorption and desorption of free phosphate on the HAP surface induced by the pH changes. These results can be used to select suitable operating conditions and, in conjunction with general empirically based guidelines available in refs. [19] and [22] and with experiments using scale-down models such as that proposed by McCue et al. [25], can be applied to extend the lifetime of CHT columns.

Acknowledgements

This research was supported by Bio-Rad Laboratories and by NSF Grant No. CTS-0729857.

References

[1] R. Giovannini, R. Freitag, Bioseparation 9 (2000) 359.
[2] R. Giovannini, R. Freitag, Biotechnol. Bioeng. 77 (2002) 445.
[3] E. Dolinski, K. Hawkins, J. Myers, Process-scale ceramic hydroxyapatite chromatography: benefits and issues, Abstracts of Papers of the American Chemical Society, 224 (2002) 318-BIOT Part 1.
[4] A. Jungbauer, R. Hahn, K. Deinhofer, P. Luo, Biotechnol. Bioeng. 87 (2004)364.
[5] P. Ng, A. Cohen, V. McLaughlin, Bioprocess Intern. 4 (2006) 46.
[6] S. Schubert, R. Freitag, J. Chromatogr. A 1142 (2007) 106.
[7] D.L. Wensel, B.D. Kelley, J.L. Coffinan, Biotechnol. Bioeng. 100 (2008) 839.
[8] P. Gagnon, New Biotechnol. 25 (2009) 287.
[9] M.J. Gorbunoff, Anal. Biochem. 136 (1984) 425.
[10] M.J. Gorbunoff, Anal. Biochem. 136 (1984) 433.
[11] M.J. Gorbunoff, Anal. Biochem. 136 (1984) 440.
[12] T. Kawasaki, J. Chromatogr. 544 (1991) 147.
[13] P.K. Ng, J. He, P. Gagnon, J. Chromatogr. A 1142 (2007) 13.
[14] S. Schubert, R. Freitag, J. Chromatogr. A 1216 (2009) 3831.
[15] P. Gagnon, C.-W. Cheung, P.J. Yazaki, J. Sep. Sci. 32 (2009) 3857.
[16] A.N. Smith, A.M. Posner, J.P. Quirk, J. Colloid Interface Sci. 54 (1976) 176.
[17] J.C. Gramain, J.C. Voegel, M. Gumper, J.M. Thomann, J. Colloid Interface Sci. 118 (1987) 148.
[18] T.E. Gills, National Institute of Standards & Technology, Standard Reference Material 2910–Calcium Hydroxyapatite, Gaitherburg, MS, USA, 1997.
[19] CHT® Ceramic Hydroxyapatite–Instruction Manual, Bio-Rad Laboratories, 2009.
[20] L.J. Cummings, Paper presented at SPICA 2008—Symposium on Preparative and Industrial Chromatography and Allied Techniques, Zurich, Switzerland, 2008.
[21] T.E. Bankston, L. Dattolo, G. Carta, J. Chromatogr. A. 1217 (2010) 2123.
[22] L.J. Cummings, M.A. Snyder, K. Brisack, Methods Enzymol. 466 (2009)387.
[23] L.J. Cummings, M.A. Snyder, Paper presented at Recovery of Biological Products XIV, Lake Tahoe, CA, USA, 2010.
[24] L. J. Cummings, M.A. Snyder, Paper presented at BIT Life Sciences' 2nd Annual International Congress on Antibodies, Beijing, China, 2010.
[25] J.T. McCue, D. Cecchini, K. Hawkins, E. Dolinski, J. Chromatogr. A 1165 (2007) 78.